Supplement of Solid Earth, 10, 2045–2072, 2019
https://doi.org/10.5194/se-10-2045-2019-supplement

Supplement of

Tectonic processes, variations in sediment flux, and eustatic sea level recorded by the 20 Myr old Burdigalian transgression in the Swiss Molasse basin

Philippos Garefalakis and Fritz Schlunegger

Correspondence to: Philippos Garefalakis (philippos.garefalakis@geo.unibe.ch)

S1 Reconstructions of palaeo-bathymetrical conditions

S1.1 Reconstruction of the water depth from ripple-marks morphometry and grain size

The palaeo-bathymetrical conditions were derived from sedimentary structures such as symmetric- and asymmetric-ripple-marks. These bedforms need bottom oscillatory waves to form (Komar and Miller, 1973). Accordingly, the morphometry and grain side of these bedforms bear information about the velocity of the oscillatory currents, which can be used as basis to calculate palaeo-water depth conditions (Allen, 1981). In addition, the orientation of asymmetric ripple-marks and preserved ripple-crests allow to interpret the flow direction and the orientation of the coastline during their formation (Clifton and Dingler, 1984).

In the past years, several authors have used field-based data on the spacing λ, the height h and the median grain size D of oscillatory ripple-marks in various environments to estimate of palaeo-wave conditions (e.g. Tanner, 1971; Komar and Miller, 1973; Allen, 1981; Clifton and Dingler, 1984; Diem, 1985). This has also been the case for the Swiss Molasse basin, where the theory of deepwater waves has served as basis to successfully calculate the palaeo-water depths based on ripple-mark morphometries (Allen, J., 1984; Allen, 1981, 1984, 1997; Allen et al. 1985; Diem, 1985). Here, the focus lies on vortex ripples, which have a steepness of $h/\lambda < 0.12\text{-}0.22$ (Clifton and Dingler, 1984) or a VFI of $\lambda/h < 7.5 << 10$ (Allen, P., 1984) and which were likely formed by waves.

The ripple spacing λ depends on the near-bed orbital diameter d_o, which decreases exponentially with water depth (Allen, P. 1984, Allen, J., 1984; Miller and Komar, 1980a and 1980b; Fig. S3):

$$d_o = \lambda/0.65 \qquad (1).$$

Measurements of the grain size D allow calculations of the critical velocity for sediment entrainment U_t, where variations in D need to be considered (Komar and Miller, 1973):

$$For\ D < 0.5mm;\ \ U_t^{\,2} = 0.21\,(d_o/D)^{1/2}\,\frac{(\rho_s - \rho_w)gD}{\rho_w} \qquad (2a),$$

$$For\ D \geq 0.5mm;\ \ U_t^{\,2} = 0.46\pi\,(d_o/D)^{1/4}\,\frac{(\rho_s - \rho_w)gD}{\rho_w} \qquad (2b).$$

Here, the variables ρ_s and ρ_w denote the sediment and water densities, respectively, and g refers to the gravitational acceleration. The maximum wave period T_{max} can then be calculated using the estimates of the near-bed orbital diameter d_o and the threshold velocity U_t for sediment entrainment (Allen, P., 1984):

$$T_{max} = \pi d_0 / U_t \quad (3).$$

The wave period allows to calculate the deep-water wavelength L, which is independent of the water depth and bases on the wave period only (Allen, P., 1984):

$$L = T^2{}_{max} \frac{g}{2\pi} \quad (4).$$

Allen (1997) suggests that orbital diameters of oscillatory water particles decrease exponentially from the surface to greater water depths, where:

$$d_y = H \exp(y \frac{2\pi}{L}) \quad (4),$$

where d_y is the orbital diameter at a specific water depth ($-y$, negative term), H is the wave height, and L is the wavelength (all in m), respectively. Similar to the diameter, the maximum orbital velocity of water particles c_y also decreases with water depth (Allen, 1997):

$$c_y = A \frac{2\pi}{L} c_{y=0} \exp(y \frac{2\pi}{L}) \quad (5),$$

where A is the amplitude equal to the half of the waveheight H and $c_{y=0}$ is the celerity (wave propagation velocity in m/s) of deep-water waves at the surface, respectively (Fig. S3). According to Allen, P. (1984) the celerity at the surface ($c_{y=0}$) can be calculated through:

$$c_{y=0} = \sqrt{\frac{gL}{2\pi}} = \frac{L}{T}. \quad (6).$$

Since A in Eq. (5) refers to the half of the waveheight H, we can substitute A with $H/2$. Note, that at the surface, the form of deep-water waves is not expressed as perfect semicircles in height and diameter. This is particularly the case for shallow marine environments where the waves show a flattened, elliptical shape, which reduces the height of A and eventually elongates the diameter d_0 (Fig. S3, Clifton and Dingler, 1984). We further consider the relationships between waveheight H and wavelength

L, which can be expressed through the height to length ratio $H/L = 0.142$ (Michell, 1893). By replacing H with $0.142*L$ and substituting $c_{y=0}$ with L/T Eq. (5) changes to:

$$c_y = \frac{0.142\,L}{2} * \frac{2\pi}{L} * \frac{L}{T} * \exp(y\,\frac{2\pi}{L}) = 0.142\,\pi\,\frac{L}{T}\exp(y\,\frac{2\pi}{L}) \quad (7).$$

The water depth y can then be calculated using U_t as proxy for c_y, and through the combinations of Eq. (3) and Eq. (7). This results in an expression, where the water depth y for a wave with a length L can be estimated. Since our approach mainly involves threshold conditions and maximum values, the water depth will be overestimated. Accordingly, Eq. (8) returns maximum value for palaeo-water depth:

$$y = \frac{L}{2\pi} * \ln(\frac{d_0}{0.142*2*L}) \quad (8).$$

We thus measured the ripple-spacing (λ, crest to crest), the ripple-height (h, trough to crest) and the median grain size (D) in the field. We tested whether the ratio-values of the ripple-steepness h/λ (Sleath, 1976; Miller and Komar, 1980a; Clifton and Dingler, 1984) and inversely, the ripple-index or the vertical from index VFI (Allen, P., 1984; Allen, J. 1979), fulfilled the criteria for vortex ripples. We then applied Eq. (9) to these 12 measurements of ripple-marks at the different sections. We justify the selection of deep-water wave theories because we focussed on those oscillation-ripple-marks (Sos-facies), which were formed in the lower shoreface where related conditions are likely to apply. The results revealed changes in bathymetrical conditions through time which were used to reconstruct the ancient sea conditions in the Molasse basin.

S1.2 Estimations of palaeo-water depth from set-thickness

We use the set-thickness of preserved sedimentary bedforms to estimate the palaeo-water depth conditions during deposition of the OMM. We mainly focus on cross-bedded- (Sc, Sct_a) and trough cross-bedded-sandstones (Sct_r) since these facies assemblages are commonly found in the OMM-deposits and they have intensely been investigated in the past by several authors (e.g. Allen, J. 1982; 1984; Allen, P., 1984; Rust and Gibling, 1990; Nicholson, 1993; Bridge and Tye, 2000; Mohrig et al., 2000; Leclair and Bridge, 2001; Tjerry and Fredsøe, 2005; Hajek and Heller, 2012; Blondeaux and Vittori, 2016). We use the fact, that according to these authors the bedform thickness h_b and the mean water depth y_m are positively correlated to each other. Furthermore, in the case of tabular cross-beds (Sct_a), which we interpret as sandwaves, the water depth during their formation is directly proportional to their height (e.g. Blondeaux and Vittori, 2010). In this case, the properties of sandwaves explored by Yalin (1964; 1992) returned a relationship between the mean water depth (y_m) and the mean height of the sandwave (h_b) of approximately $y_m/h_b = 6$. Values proposed by Yalin (1964) and Allen, J. (1982; 1984), who both stated that set-thickness is increasing with water depth, resulted in the relation of $h_b/y_m = 0.1$ *to* 0.167, however with a large scatter of the plotted data.

We note, however, that other authors (e.g. Stride, 1970) contested the statement of a correlation between the height of sandwaves and the mean water depth. In addition, Flemming (2000) also refuted the inference that the bedform height is only depending on the water depth. Instead he showed that grain-size and flow-velocity also plays a primary role in the formation of sandwaves with various heights. Nevertheless, it is possible to estimate minimum water depth levels by considering the thickness of set-heights, because the minimum water depth must be at least as high as the preserved set-thickness. We thus proceeded following the approach by Bridge and Tye (2000), who explored sandy river dunes where the sedimentary properties are similar to those of marine sandwaves (e.g. Allen, J., 1984; Hulscher and Dohmen-Janssen, 2005) encountered in our sections. These authors proposed that the relationship between the mean water depth and mean dune height ranges in average between 6 and 10 (Bridge and Tye, 2000), which is confirmed by the study of Leclair and Bridge (2001). In addition, we need to consider that these relationships do not include post-depositional erosion or compaction of the bedforms, which accordingly results in an underestimation of the palaeo-water depth.

In summary, we used the aforementioned relationships in order to estimate the range of the paleo-water depth (y_m) from the preserved set-height (h_b) of cross-beds (Sc) and dunes (Sct_a, Sct_r) by applying the relationship of Allen, J. (1982) and Bridge and Tye (2000), which are summarized in Eq. (1) and Eq. (2), alternatively:

$$y_{m1} = h_b / \, 0.1 \ to \ 0.167 \qquad \text{after Allen, J. (1982)} \qquad (1),$$

$$y_{m2} = h_b * 6 \ to \ 10 \qquad \text{after Bridge and Tye (2000)} \qquad (2).$$

The results of our palaeo-bathymetric estimations are presented as plots in the sedimentological profile sections (Figs. 4, see manuscript) and as numerical data in Table S2 (Entlen) and Table S3 (Sense), respectively. Calculations of cross-beds thickness of inferred sand-waves are shown Table S1 together with already published data from the Swiss Molasse basin.

References

Allen, J.R.L. : A model for interpretation of wave ripple-marks using their wavelength, textural composition, and shape. J. geol. Soc. London, 146. 673 – 682, 1979.

Allen, J.R.L. : Sedimentary Structures. Their Characteristics and Physical Basis. Vol. I. Developments in Sedimentology 30A. Elsevier, Amsterdam, 593 p., 1982.

Allen, J.R.L. : Sedimentary Structures. Their Characteristics and Physical Basis. Vol. I. Developments in Sedimentology 30B. Elsevier, Amsterdam, 679 p., 1984.

Allen, P.A. : Earth Surface Processes, 404 p. ISBN 0-632-03507-2, 1997.

Allen, P.A. : Some Guidelines In Reconstructing Ancient Sea Conditions From Wave Ripplemarks. Marine Geology, 43, 59 – 67, 1981.

Allen, P.A. : Reconstruction of ancient sea conditions with an example from the Swiss Molasse. Marine Geology 60, 455 – 473, 1984

Allen, P. A., and Homewood, P. : Evolution and mechanics of a Miocene tidal sandwave. Sedimentology, 31 (1), 63 – 81, 1984.

Allen, P.A., Mange-Rajetky, A. and Matter, A. : Dynamic palaeogeography of the open Burdigalian seaway, Swiss Molasse basin. Eclogae Geologicae Helvetia 78, 351 – 381, 1985.

Blondeaux, P. and Vittori, G. : A model to predict the migration of sand waves in shallow tidal seas. Continental Shelf Research, 112, 31 – 45, 2016.

Bridge, J.S. and Tye, R.S. : Interpreting the dimensions of ancient fluvial channel bars, channels and channel belts from wireline-logs and cores. AAPG Bulletin, 84 (8), 1205 – 1228, 2000.

Clifton, H.E. and Dingler, J.R. : Wave-Formed Structures and Paleoenvironmental Reconstruction. Marine Geology, 60, 165 – 198, 1984.

Diem, B. : Analytical method for estimating paleowave climate and water depth from wave ripple marks. Sedimentology, 32, 705 – 720, 1985.

Flemming, B. : The role of grain size , water depth and flow velocity as scaling factors controlling the size of subaqueous dunes. Marine Sandwave Dynamics, 23 & 25, 55 – 61, 2000.

Hajek, E.A. and Heller, P.L. : Flow-Depth Scaling In Alluvial Architecture and Nonmarine Sequence Stratigraphy: Example from the Castlegate Sandstone, Central Utah, U.S.A. Journal of Sedimentary Research, 82 (2), 121 – 130, 2012.

Hulscher, S.J.M.H. and Dohmen-Janssen, C.M. : Introduction to special section on Marine Sand Wave and River Dune Dynamics. Journal of Geophysical Research, 110, 1 – 6, 2005.

Keller, B. : Fazies und Stratigraphie der Oberen Meeresmolasse (Unteres Miozän) zwischen Napf und Bodensee. Ph.D., Bern, 302 p., 1989.

Komar, P.D. and Miller, M.C. : The threshold of sediment movement under oscillatory water waves. 43 (4), 1101 – 1110, 1973.

Leclair, S.F. and Bridge, J.S. : Quantitative interpretation of sedimentary structures formed by river dunes. Journal of Sedimentary Research, 71, 713 – 716, 2001.

Michell, M.A. : The highest Waves in Water. The London, Edinbrugh, and Dublin Philosophical Magazine and Journal of Science, 36 (5), 430 – 437, 1893.

Miller, M.C. and Komar, P.D. : Oscillation Sand Ripples Generated by Laboratory Apparatus. Journal of Sedimentary Research, 50(1), 173 – 182, 1980a.

Miller, M.C. and Komar, P.D. : A field investigation of the relationship between oscillation ripple spacinng and the near-bottom water orbital motions. Journal of Sedimentary Research, 50 (1), pp.183 – 191, 1980b.

Mohrig, D., Heller, P.L., Paola, C. and Lyons, W.J. : Interpreting avulsion process from ancient alluvial sequences: Guadalope-Matarranya system (northern Spain) and Wasatch Formation (western Colorado). GSA Bulletin, 112 (12), 1787 – 1803, 2000.

Nicholson, P.G. : A basin reappraisal of the Proterozoic Torridon Group, northwest Scotland. Spec. Publs. Int. Ass. Sediment 20, 183 – 202, 1993.

Rust, B.R. and Gibling, M.R. : Braidplain evolution in the Pennsylvanian South Bar Formation, Sydney basin, Noca Scotia, Canada. Journal of Sedimentary Petrology, 60 (1), 59 – 72, 1990.

Schaad, W., Keller, B. and Matter, A. : Die Obere Meeresmolasse (OMM) am Pfänder: Beispiel eines Gilbert-Deltakomplexes. Eclogae Geologicae Helvetiae, 85, 145 – 168, 1992.

Sleath, J.F.A. : On rolling grain ripples. J. Hydraul. Res., 14, 69 – 80, 1976.

Stride, A. H. : Shape and size trends for sandwaves in a depositional zone of the North Sea. Geol. Mag. 107, 469 – 477, 1970.

Tanner, W.F. : Numerical estimates of ancient waves, water depth and fetch. Sedimentology, 16, 71 – 88, 1971.

Tjerry, S. and Fredsøe, J. : Calculation of dune morphology. Journal of Geophysical Research, 110, 13 p., 2005.

Yalin, M.S. : Geometrical properties of sand waves. Journal of the Hydraulics Division, ASCE, 90, 105 – 119, 1964.

Yalin, M.S. : River Mechanics. Pergamon Press, Oxford, 219 p., 1992.

Table S1: Estimates of water depths from preserved cross-bed thickness at various sites

Unit	*Site (this study) (see Fig. 2a)*	*Water depth (this study)*	*Water depth and location (other studies)*
c. OMM-Ib (?)	*Marly*	*12 – 20 m*	*10 m, Marly (Allen and Homewood, 1984)*
c. OMM-Ib (?)	*St. Magdalena*	*3 – 5 m*	
OMM-Ib	*Estavayer-le-Lac*	*30 – 50 m*	
OMM-Ib	*Mägenwil*	*36 – 60 m; up to 100 m in places*	*25 – 60 m, Mägenwil (Allen and Homewood, 1984)*
OMM-Ib (?)			*10 – 35 m, Bay near Napf (Keller, 1989)*
OMM-II			*20 m, Pfänder-Delta (Schaad et al., 1992)*

Table S2: Estimates of water depths from preserved cross-bed thickness at the Entlen section

Unit	*Stratigraphic level (approx.)*	*Water depth (this study)*
OMM-Ia	*10 m*	*1.3 – 2.2 m*
	50 m	*1.7 – 2.9 m*
	60 m	*0.7 – 1.2 m*
	80 m	*1.2 – 2.1 m*
	90 m	*1.1 – 1.9 m*
	190 m	*1.4 – 2.4 m*
	230 m	*1.0 – 1.8 m*
	280 m	*0.8 – 1.3 m*
	290 m	*1.5 – 2.5 m*
OMM-Ib	*370 m*	*12 – 20 m*
	390 m	*4.4 – 7.3 m*
	420 m	*0.15 – 0.35 m*
	420 m	*0.2 – 0.35 m*
	430 m	*0.10 – 0.2 m*
	430 m	*0.1 – 0.35 m*
	650 m	*3.3 – 5.5 m*
	660 m	*2.9 – 4.8 m*
	680 m	*1 – 1.8 m*
	700 m	*5 – 8.5 m*
	720 m	*6 – 10 m*

Table S3: Estimates of water depths from preserved cross-bed thickness at the Sense section

Unit	*Stratigraphic level (approx.)*	*Water depth (this study)*
OMM-Ia	*40 m*	*3 – 5 m*
	40 m	*2.4 – 4 m*
	40 m	*6.6 – 11 m*
	45 m	*2.4 – 4 m*
	45 m	*3 – 5 m*
	70 m	*1.2 – 2 m*
	75 m	*1.5 – 2.5 m*
	160 m	*2.4 – 4 m*
	170 m	*3 – 5 m*
OMM-Ib	*200 m*	*24 – 40 m*
	205 m	*15 – 25 m*
	210 m	*24 – 40 m*
	215 m	*0.07 – 0.10 m*
	220 m	*0.10 – 0.2 m*
	230 m	*1.8 – 3 m*
	235 m	*15 – 25 m*
	240 m	*0.9 – 1.5 m*
	250 m	*0.6 – 1 m*
	260 m	*0 – 1 m*

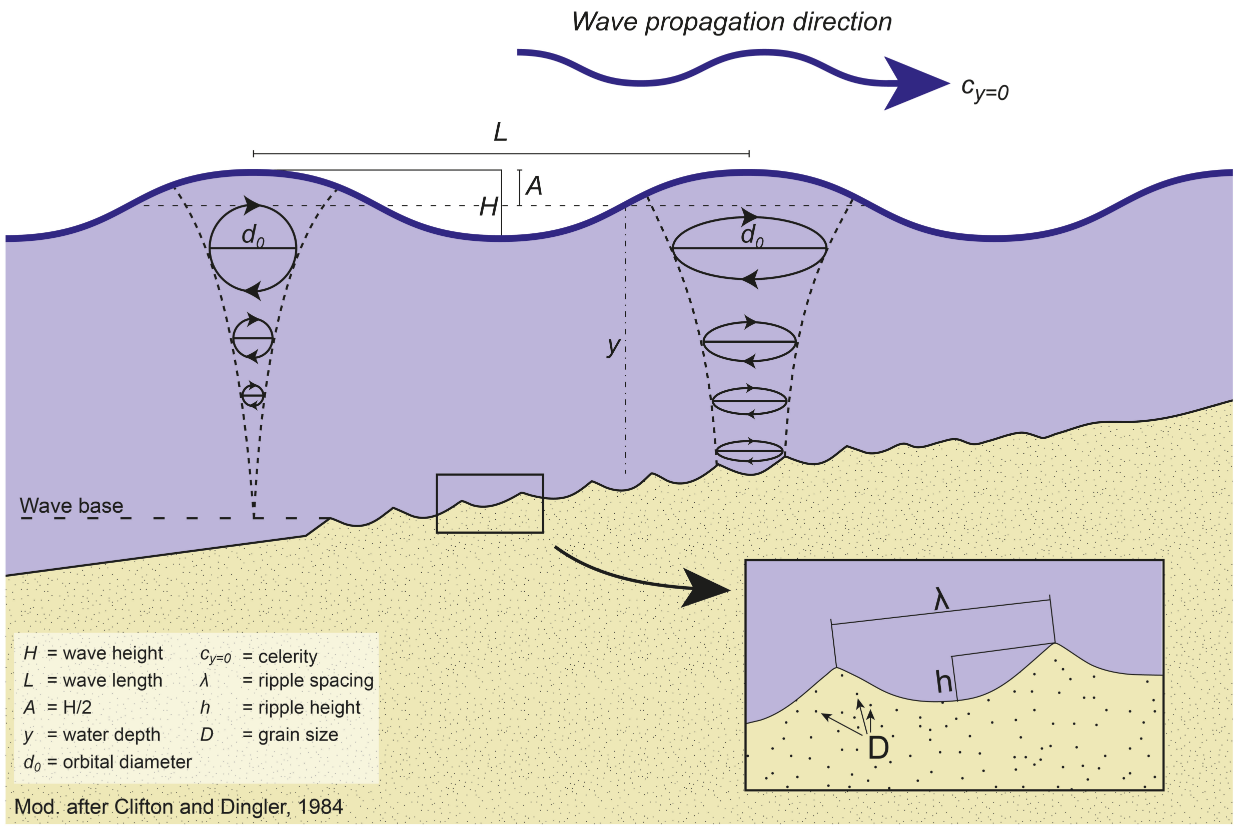

Figure S1: Schematic sketch showing important parameters of waves and wave-formed ripple marks. Note, the orbital diameter (do) refers to the wave height at the surface (H) for perfect sinusoidal shaped waves. All variables are measured in SI-units. Please see Fig. 4 for plots of the calculated water depth from oscillation-ripple-marks. Figure modified after Clifton and Dingler (1984).

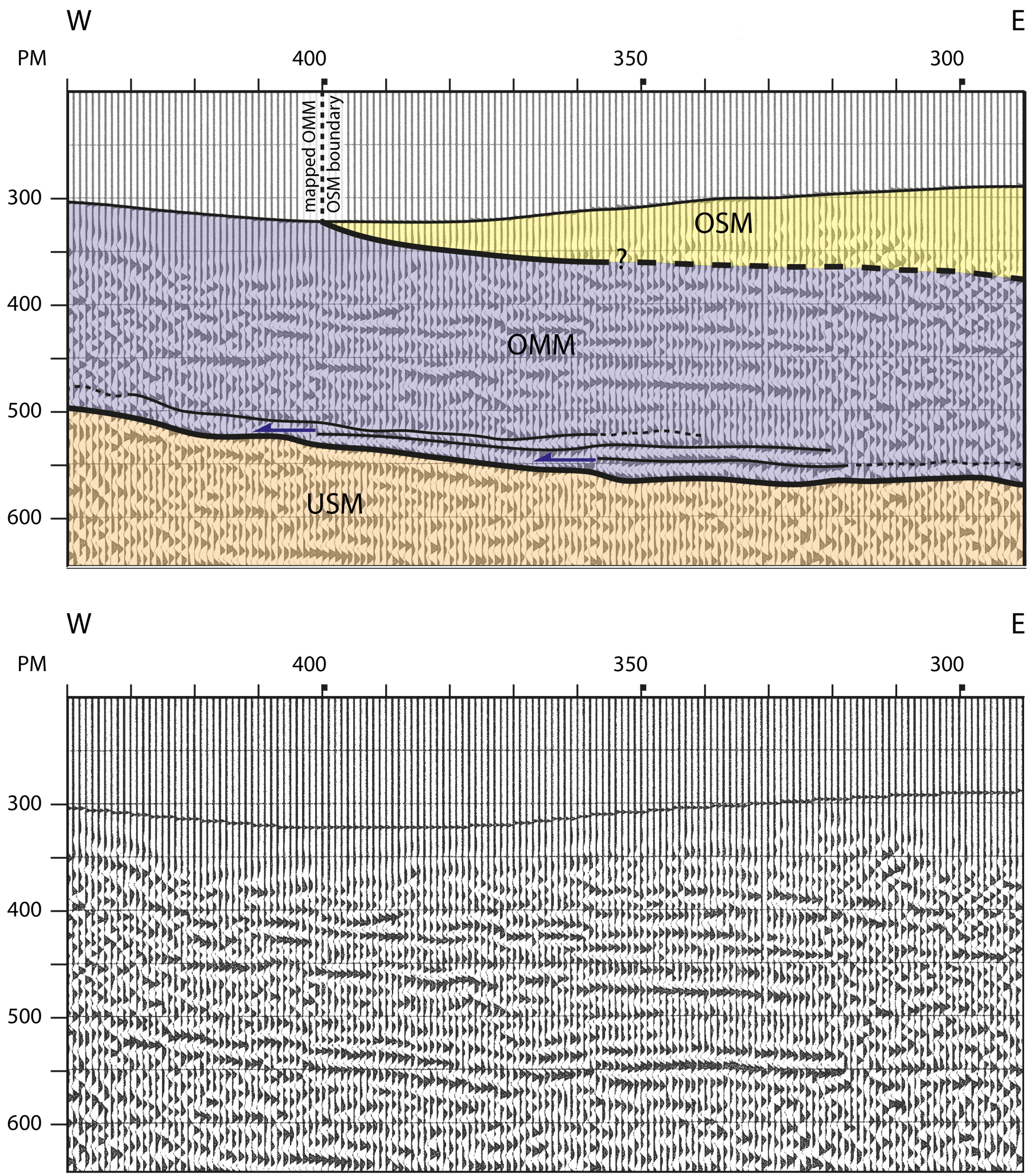

Figure S2: Seismic section BEAGBE.N780025 (courtesy SEAG, Aktiengesellschaft für Schweizerisches Erdöl, Langnau am Albis, 2019) showing the westward directed transgression of the basal OMM-deposits. Blue arrows indicate onlaps of OMM onto USM sediments. Please see Fig. 2a for trace of seismic line and see text for further discussion.

Figure S3: Photos showing the sedimentological architecture of the Gurten drillcore from top right to bottom left (courtesy Kellerhals and Haefeli AG, Geologen Bern, 2019). Please find the photos at the end of this file.

Figure S4: Photo table of sedimentary features encountered at a) the Entlen, and b) the Sense section, and from outcrops situated c) at the distal west of the basin (Heitenried,St. Magdalena and Estavayer-le-lac), and d) at the distal east of the Molasse (Madiswil, Mägenwil and the Napf). Please see Fig. 2a for location of field sites.

a1) Normal-graded sandstone with clearly visible parallel lamination (Sp).

a2) Parting lineation, equivalent to top view of a1).

a3) Cross-bedded sandstone (Sc) within massive-bedded sandstone (Sm).

a4) Climbing-ripple marks (Mcl) between massive-bedded sandstones and parallel-laminations (Sp).

a5) Pebbly lags (Sg) overlying parallel-laminations (Sp) and cross-bedded sandstones at the base.

a6) Water escape structures (sand-volcanoes, Sv) within cross- and massive-bedded sandstone (Sc, Sm).

b1) Tabular- and trough-cross beds (Sct_a, Sct_r) overlying massive-bedded sandstones (Sm). See person for scale.

b2) Current-ripple marks (Scr) draped with mudstone (Md).

b3) Detail of b2): Cross-bedded laminae of the internal Scr-structure can be used to determine the transport direction.

b4) Lenticular bedding (Mle) where sandstones are forming isolated lenses within mudstone layers.

b5) Flaser-bedding (Mlf) where sandstones are dominant and mudstones only preserved as a thin layer (Md).

c1) Estavayer-le-Lac : Meter-thick tabular-cross beds (Sct_a) at the distal western basin border. Meter stick is 2m.

c2) Heitenried : Detail of c4) – Pebbly-lags (Sg) along foresets.

c3) St. Magdalena : Trough-cross beds (Sct_r) overlying massive-bedded sandstones (Sm).

c4) Heitenried : Zoom-out of c2) – Foresets with pebbly lags (Sg) overlain by cross-bedded troughs (Sct_r, Sc).

d1) Napf : Massive conglomerates (Gm) overlying imbricated clasts at the base.

d2) Napf : Sandy foresets with pebbly-lags (Sg) among massive (Gm) and cross-bedded (Gc) conglomerates.

d3) Madiswil : Calcaerous sandstones (Scc) forming tabular cross-beds (Sct_a) of dm-height.

d4) Mägenwil : Calcaerous sandstones forming m-thick tabular cross-beds (Sct_a) at the distal basin border.

(a)

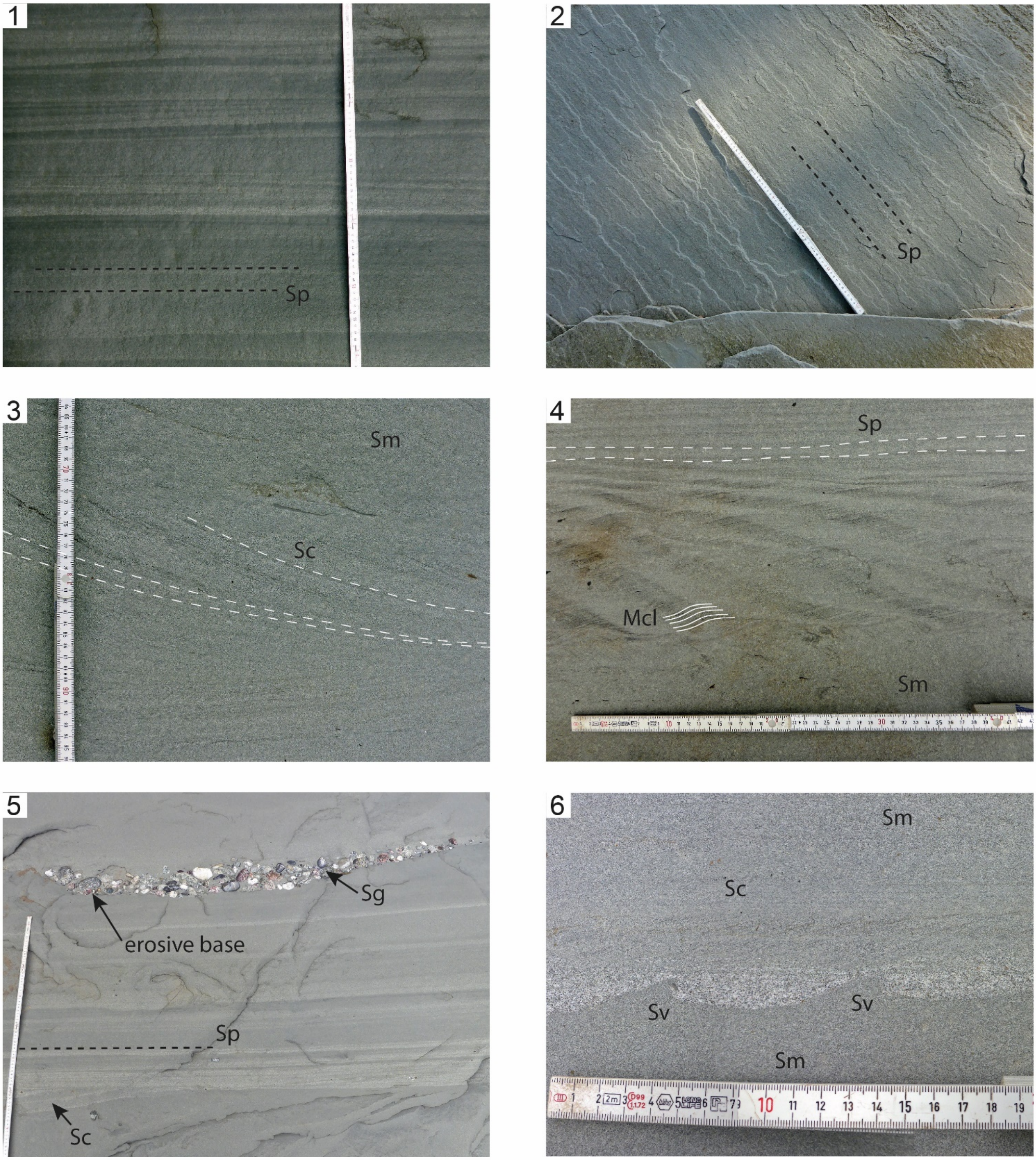

(b)

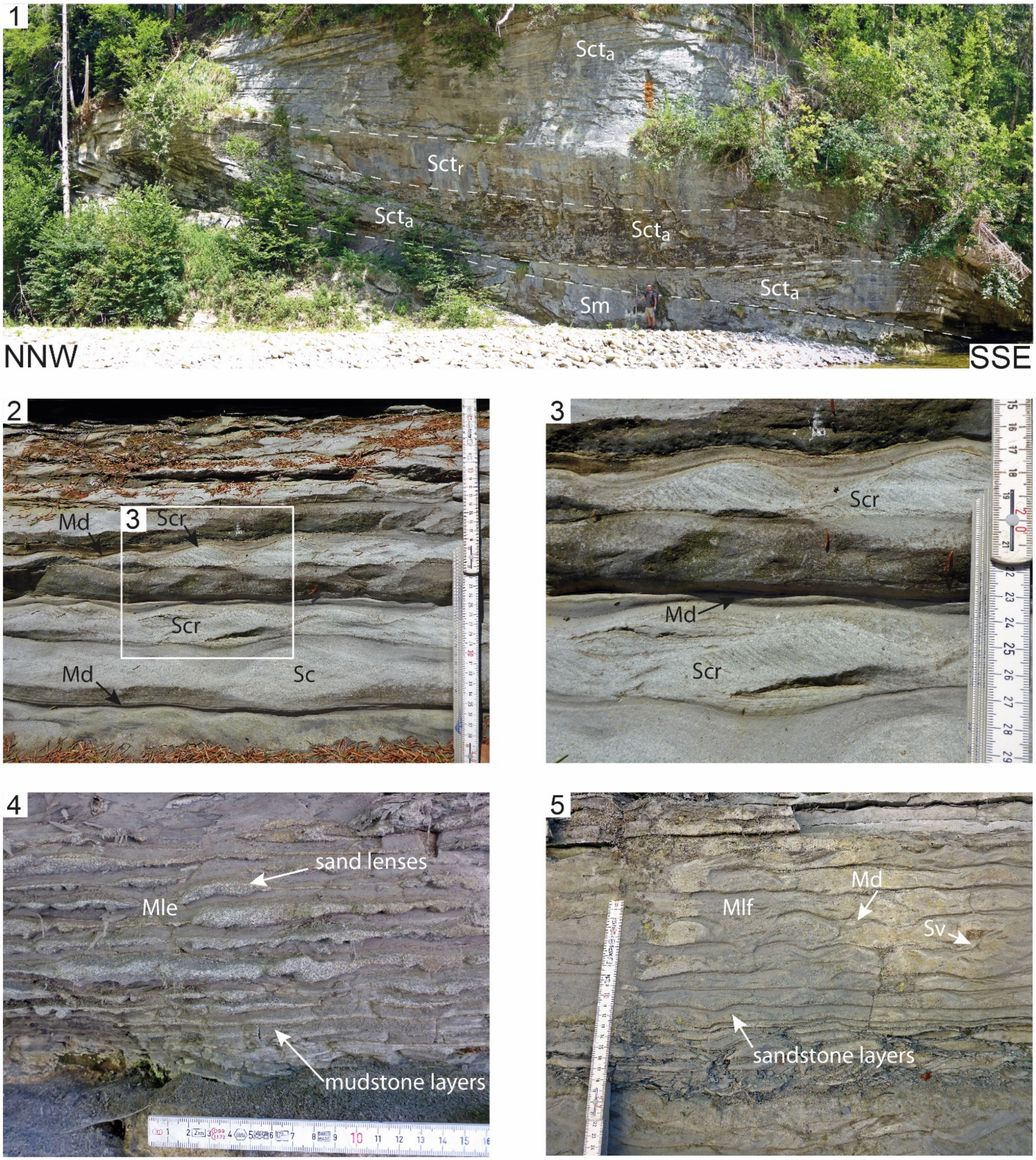
1
Sct_a
Sct_r
Sct_a
Sct_a
Sct_a
Sm
NNW
SSE
2
Md
3
Scr
Scr
Md
Sc
3
Scr
Md
Scr
4
sand lenses
Mle
mudstone layers
5
Md
Mlf
Sv
sandstone layers

(c)

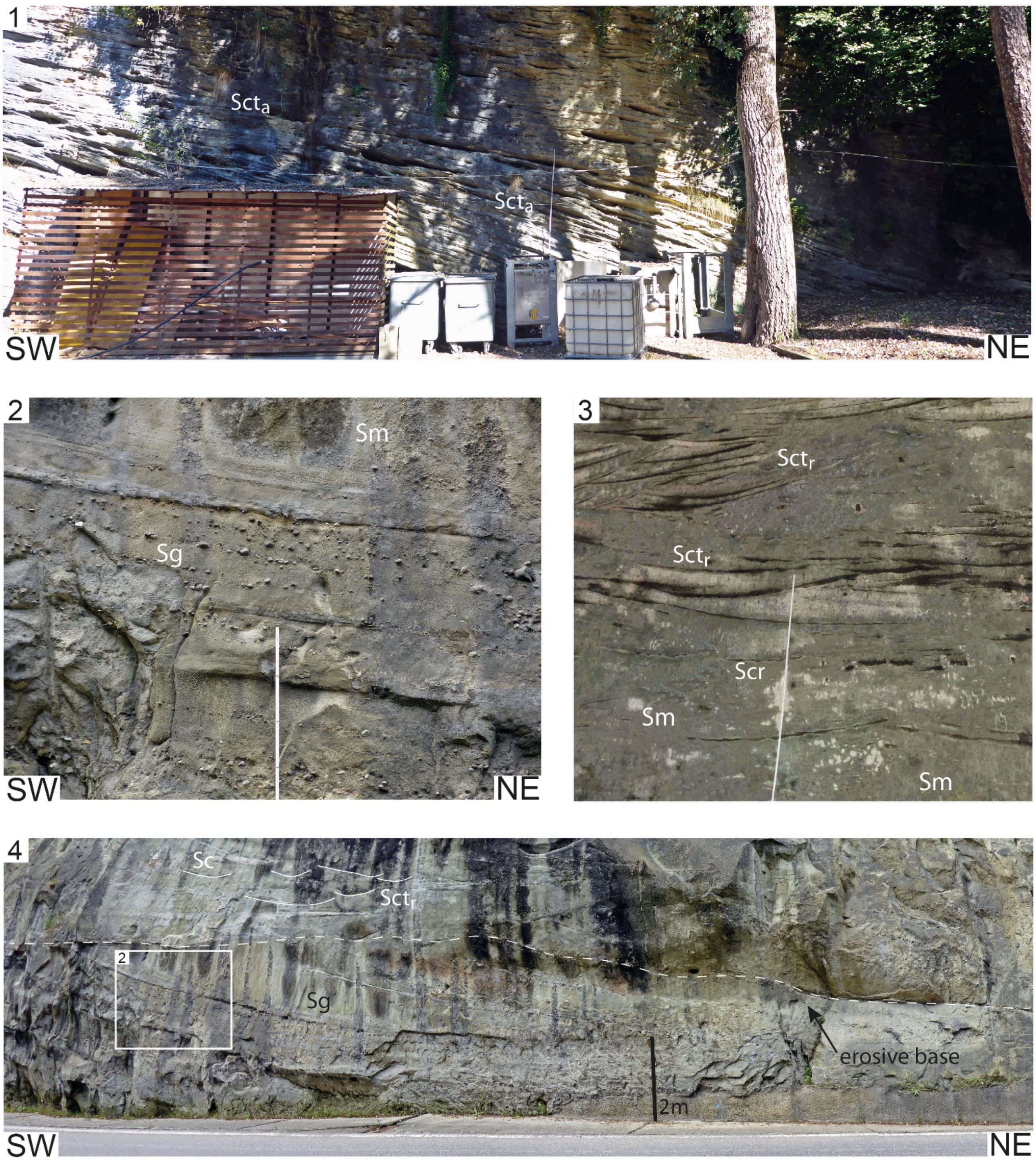
1
Sct$_a$
Sct$_a$
SW
NE
2
Sm
Sg
SW
NE
3
Sct$_r$
Sct$_r$
Scr
Sm
Sm
4
Sc
Sct$_r$
2
Sg
erosive base
2m
SW
NE

(d)

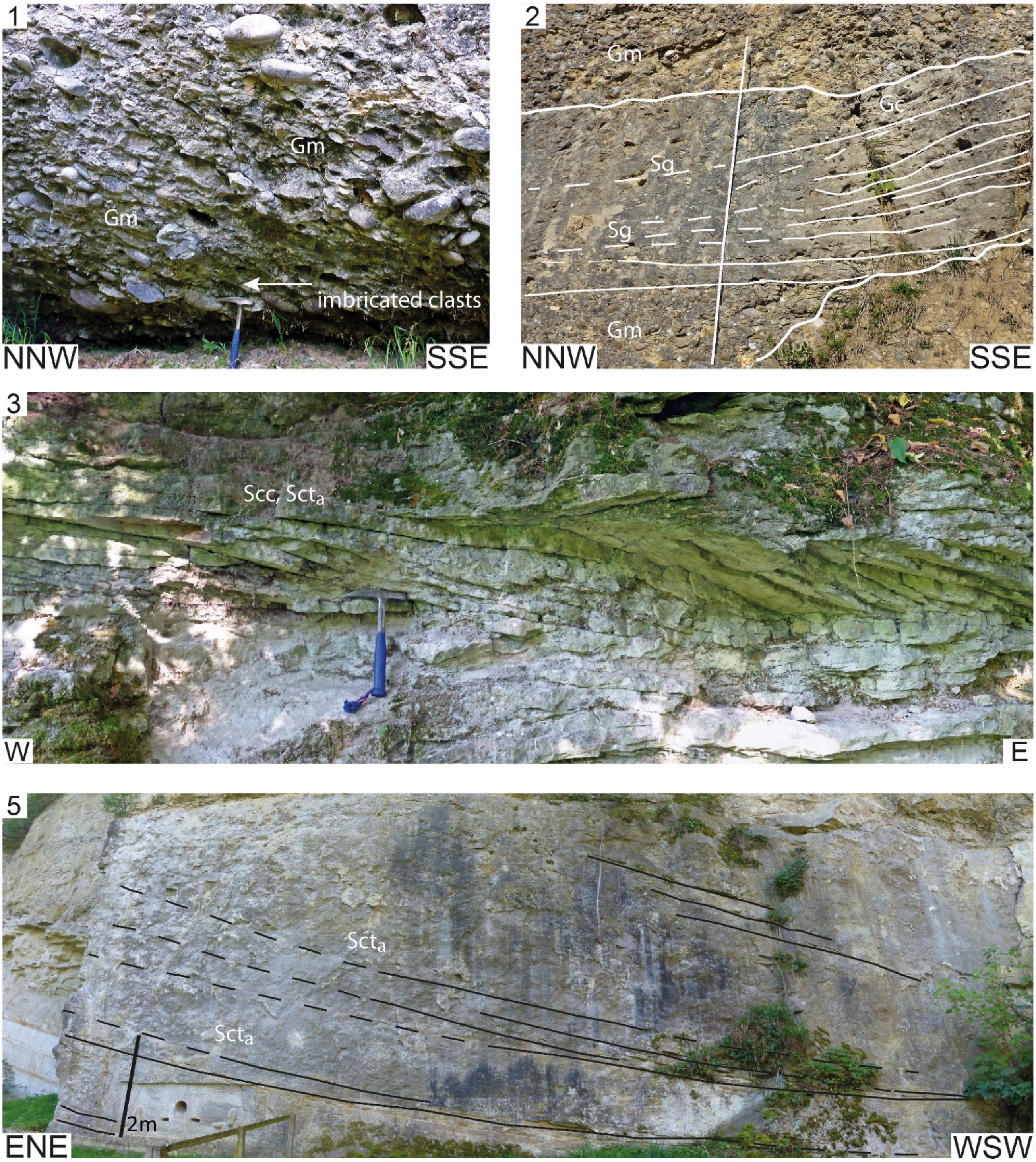
1
Gm
Gm
imbricated clasts
NNW
SSE
2
Gm
Gc
Sg
Sg
Gm
NNW
SSE
3
Scc, Sct_a
W
E
5
Sct_a
Sct_a
2m
ENE
WSW

UNIVERSITÄT BERN 1989

BOHRUNG GURTEN

UNIVERSITÄT BERN 1989

BOHRUNG GURTEN

UNIVERSITÄT BERN 1989

BOHRUNG GURTEN


UNIVERSITÄT BERN 1989
BOHRUNG
GURTEN
35
34
33
32
31
30
36
35
34
33
32
31


UNIVERSITÄT BERN 1989
BOHRUNG
GURTEN
41
40
39
38
37
36
42
41
40
39
38
37

UNIVERSITÄT BERN 1989

BOHRUNG GURTEN

BOHRUNG GURTEN

UNIVERSITÄT BERN 1989

UNIVERSITÄT BERN 1989

BOHRUNG GURTEN

59 58 57 56 55 54

60 59 58 57 56 55


UNIVERSITÄT BERN 1989
BOHRUNG
GURTEN
65 64 63 62 61 60
66 65 64 63 62 61


BOHRUNG
GURTEN
UNIVERSITÄT BERN 1989
71
70
69
68
67
66
72
71
70
69
68
67


UNIVERSITÄT BERN 1989
BOHRUNG
GURTEN
77
76
75
74
73
72
78
77
76
75
74
73


UNIVERSITÄT BERN 1989
BOHRUNG
GURTEN
83
82
81
80
79
78
84
83
82
81
80
79

BOHRUNG
GURTEN
UNIVERSITÄT BERN 1989
89
88
87
86
85
84
90
89
88
87
86
85

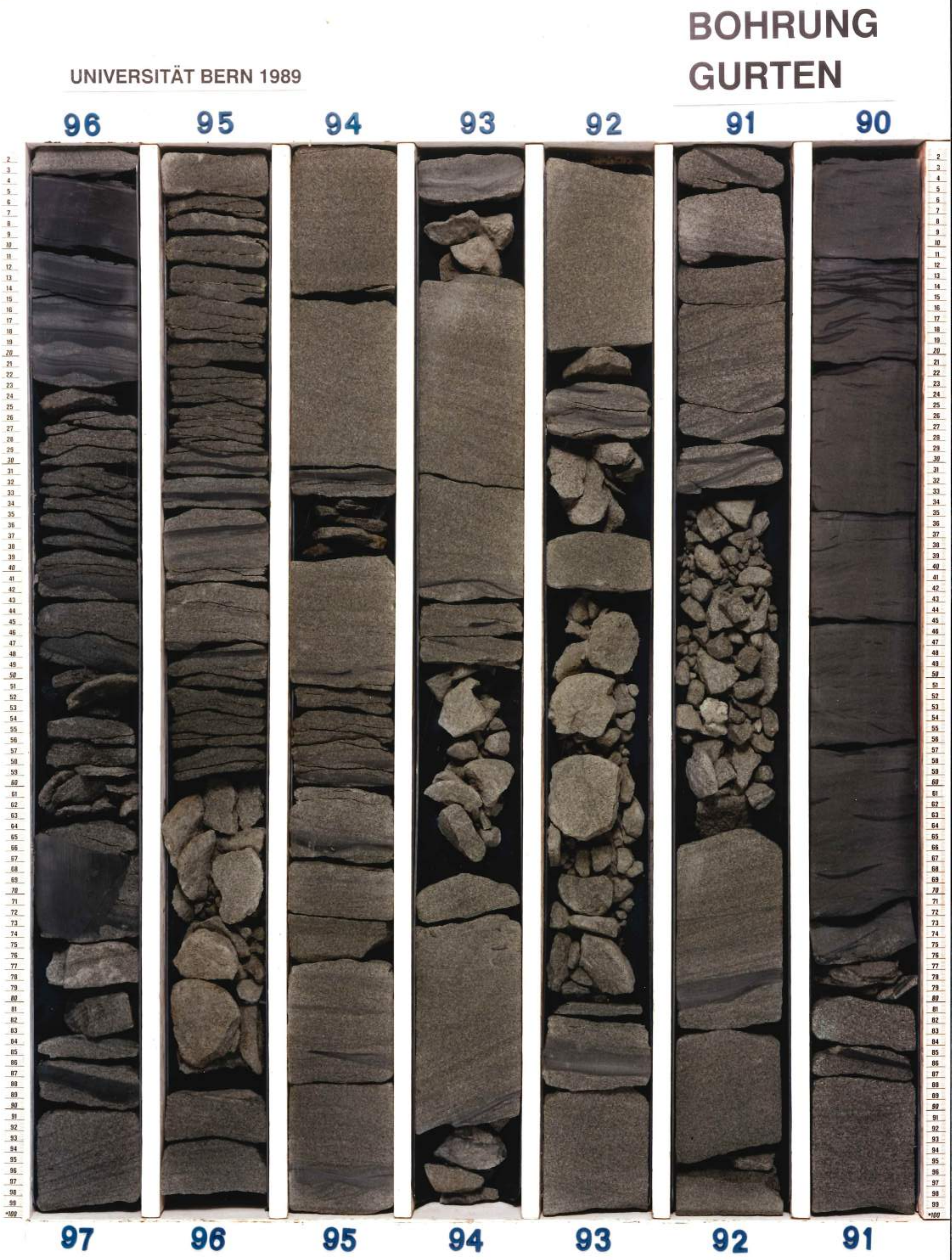
BOHRUNG
GURTEN
UNIVERSITÄT BERN 1989
96
95
94
93
92
91
90
97
96
95
94
93
92
91

BOHRUNG GURTEN

UNIVERSITÄT BERN 1989

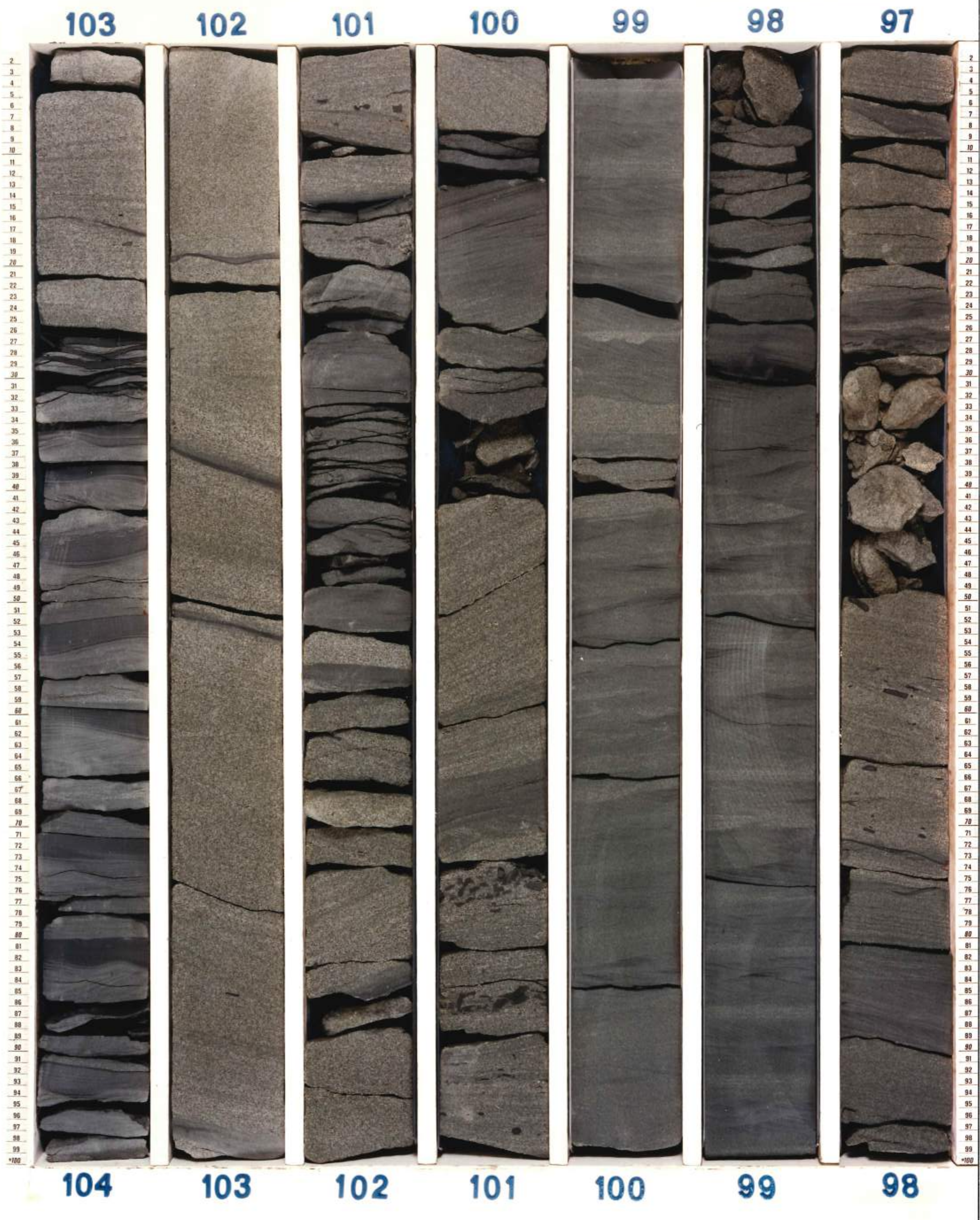

BOHRUNG
GURTEN

BOHRUNG GURTEN

BOHRUNG
GURTEN

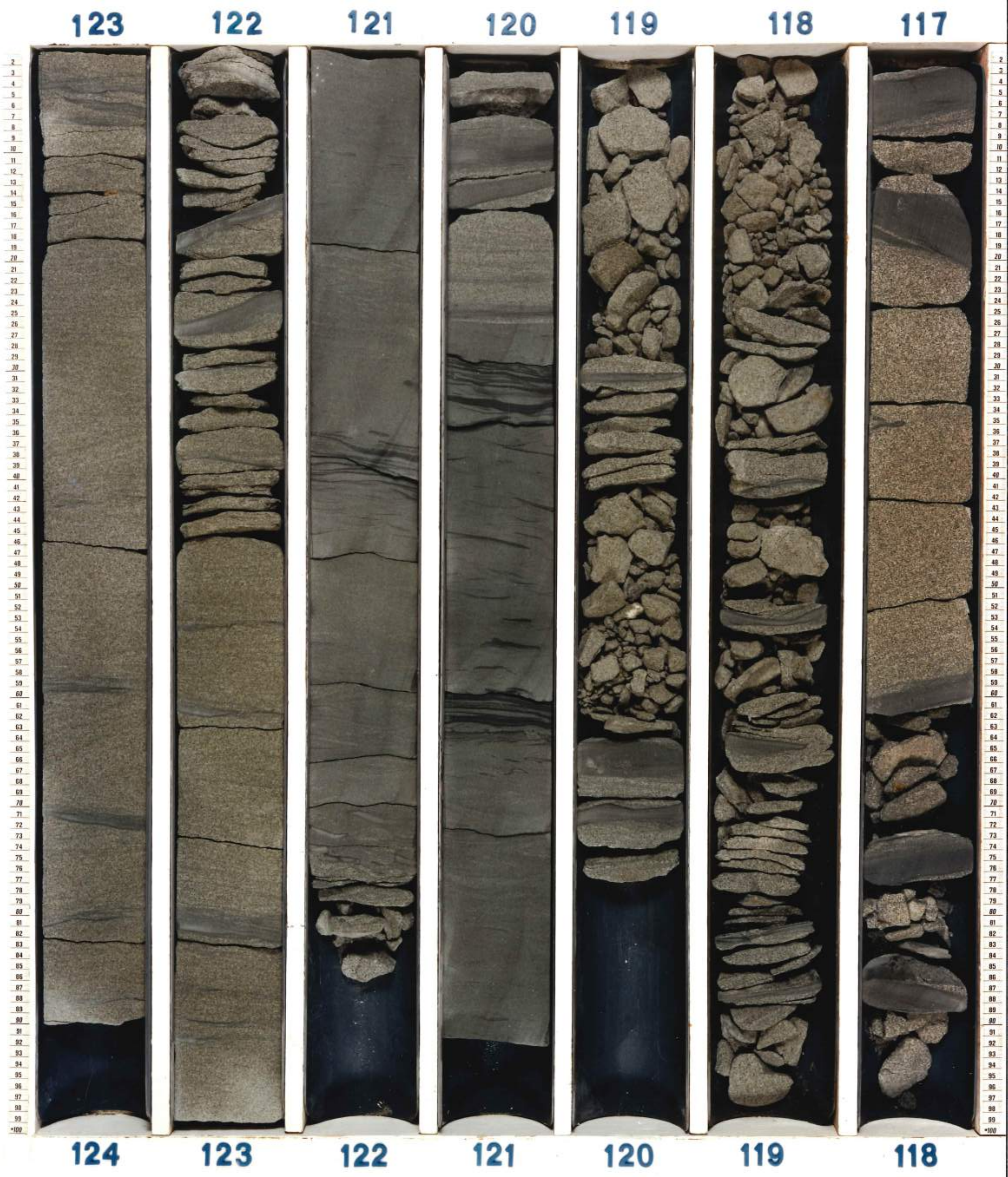

BOHRUNG GURTEN

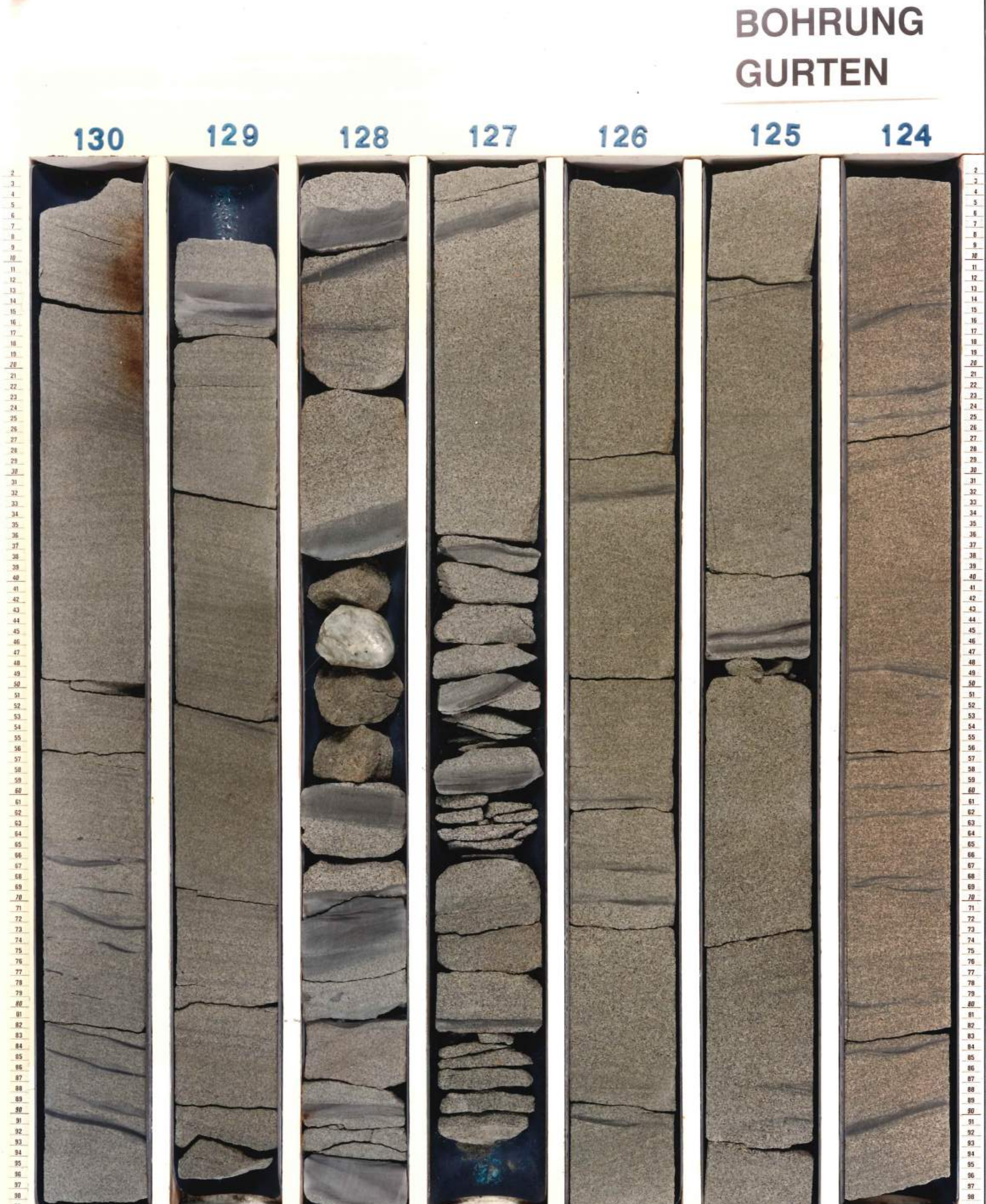

BOHRUNG
GURTEN
130
129
128
127
126
125
124
131
130
129
128
127
126
125

BOHRUNG GURTEN

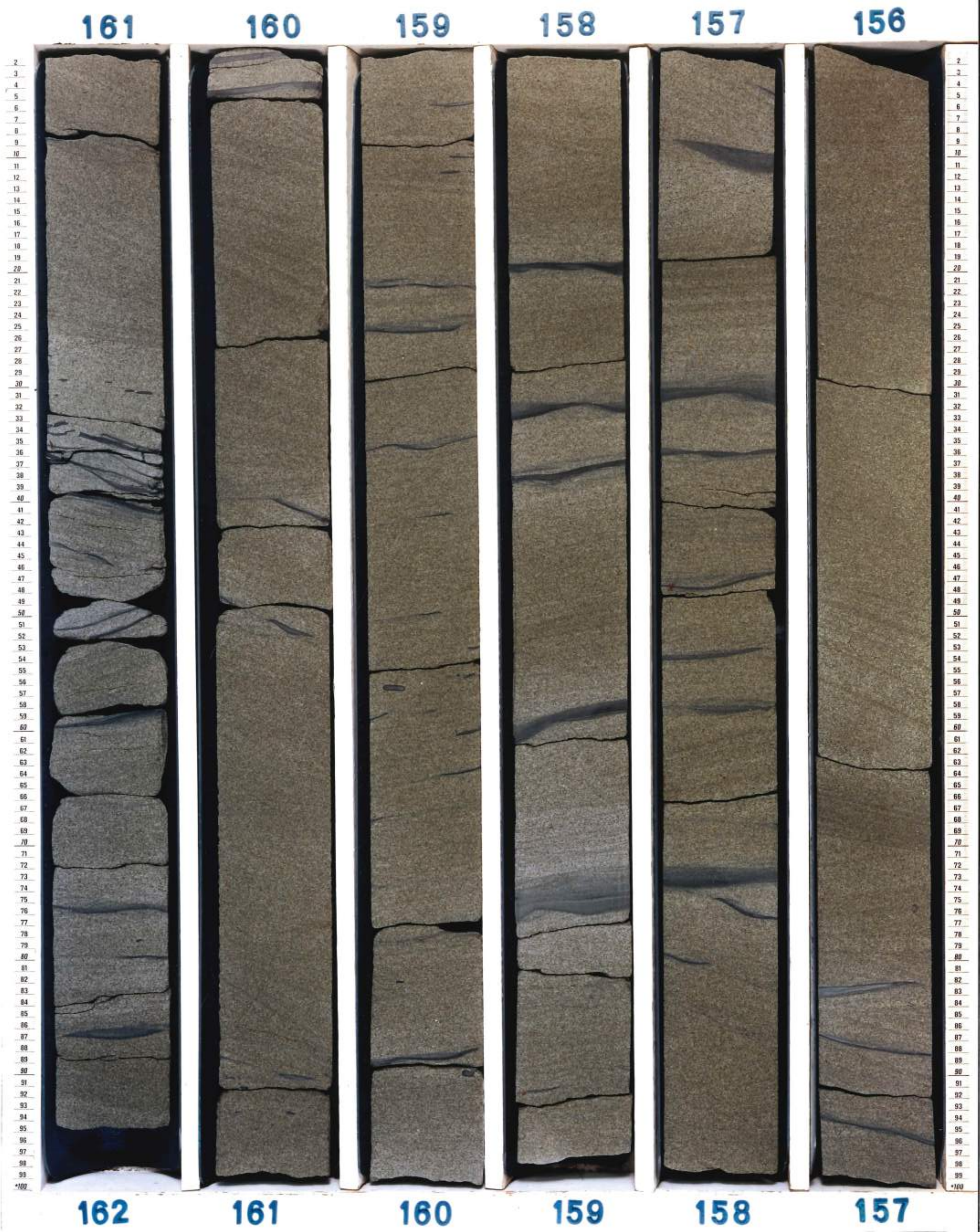

BOHRUNG
GURTEN

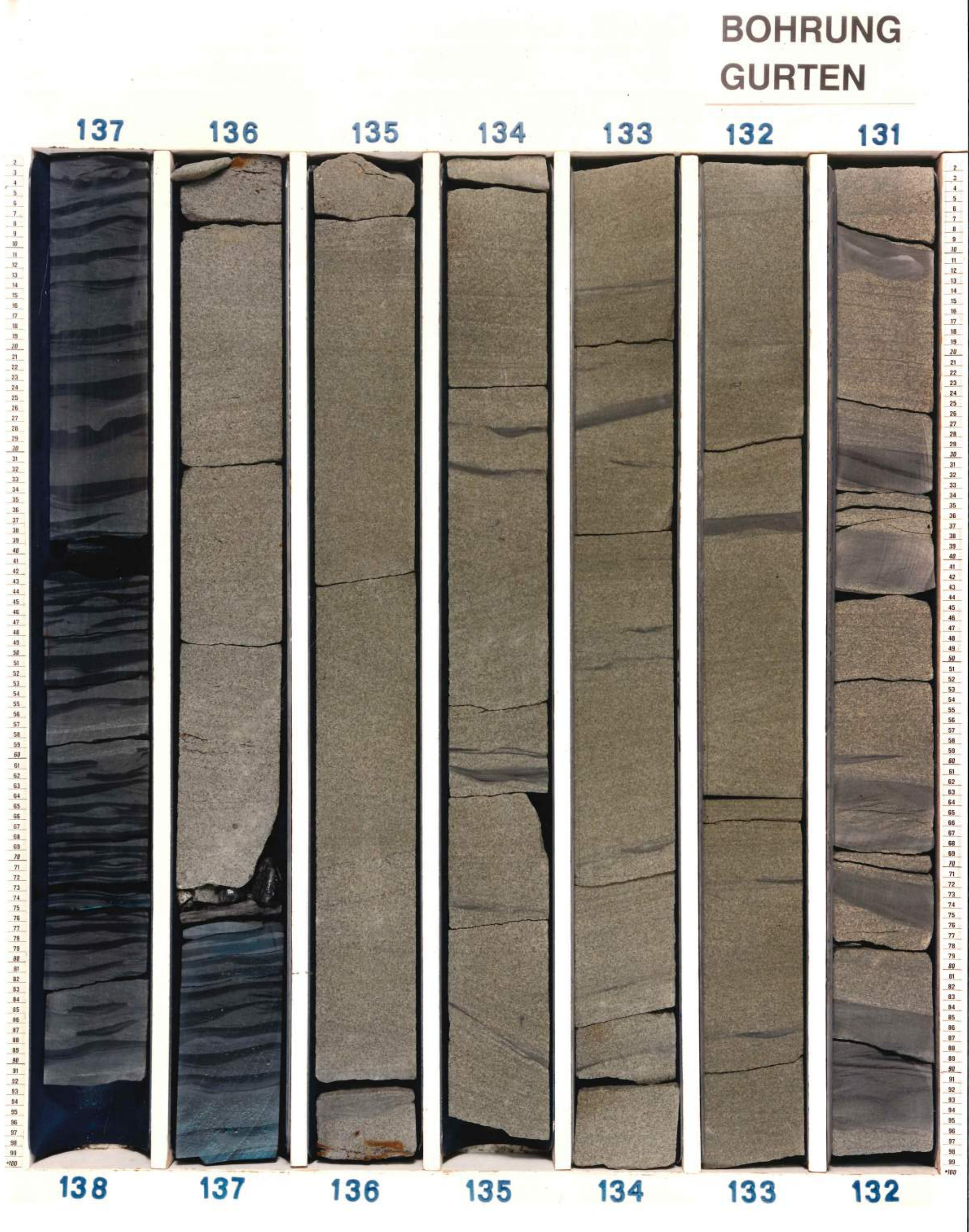
BOHRUNG
GURTEN
137
136
135
134
133
132
131
138
137
136
135
134
133
132

BOHRUNG GURTEN

BOHRUNG
GURTEN

BOHRUNG GURTEN

BOHRUNG GURTEN

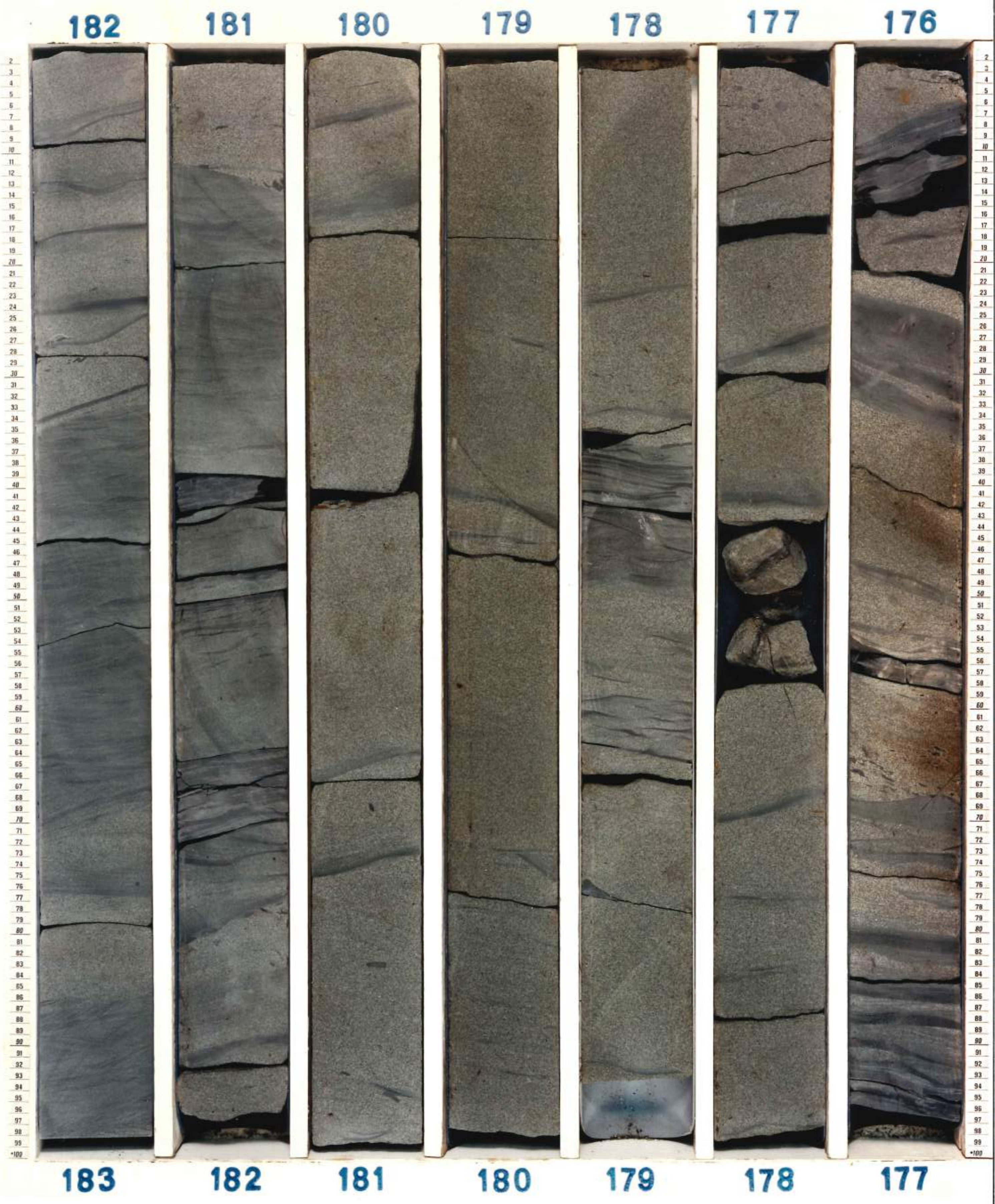

BOHRUNG GURTEN

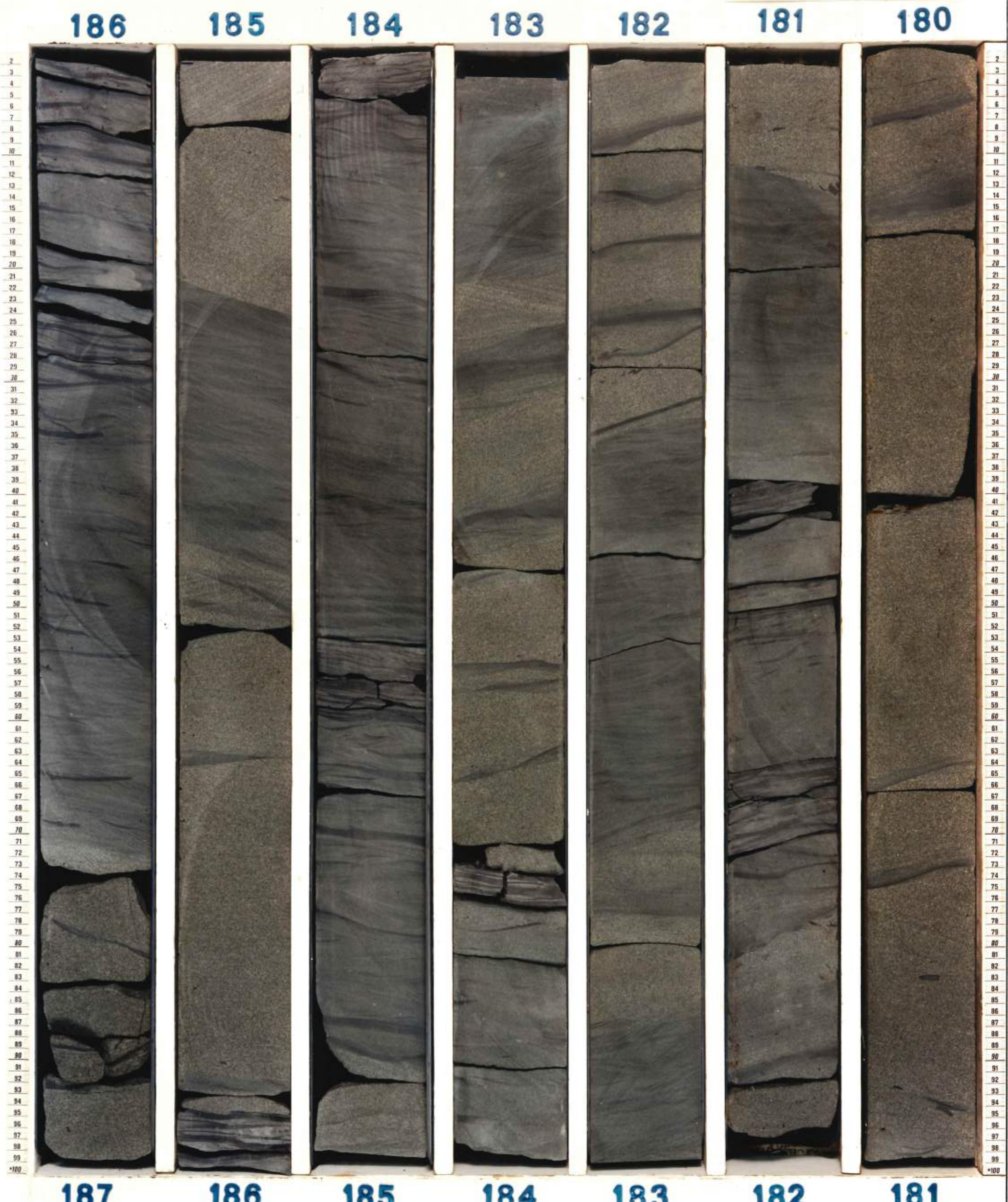

UNIVERSITÄT BERN 1989

BOHRUNG GURTEN

UNIVERSITÄT BERN 1989

BOHRUNG GURTEN

UNIVERSITÄT BERN 1989

BOHRUNG GURTEN

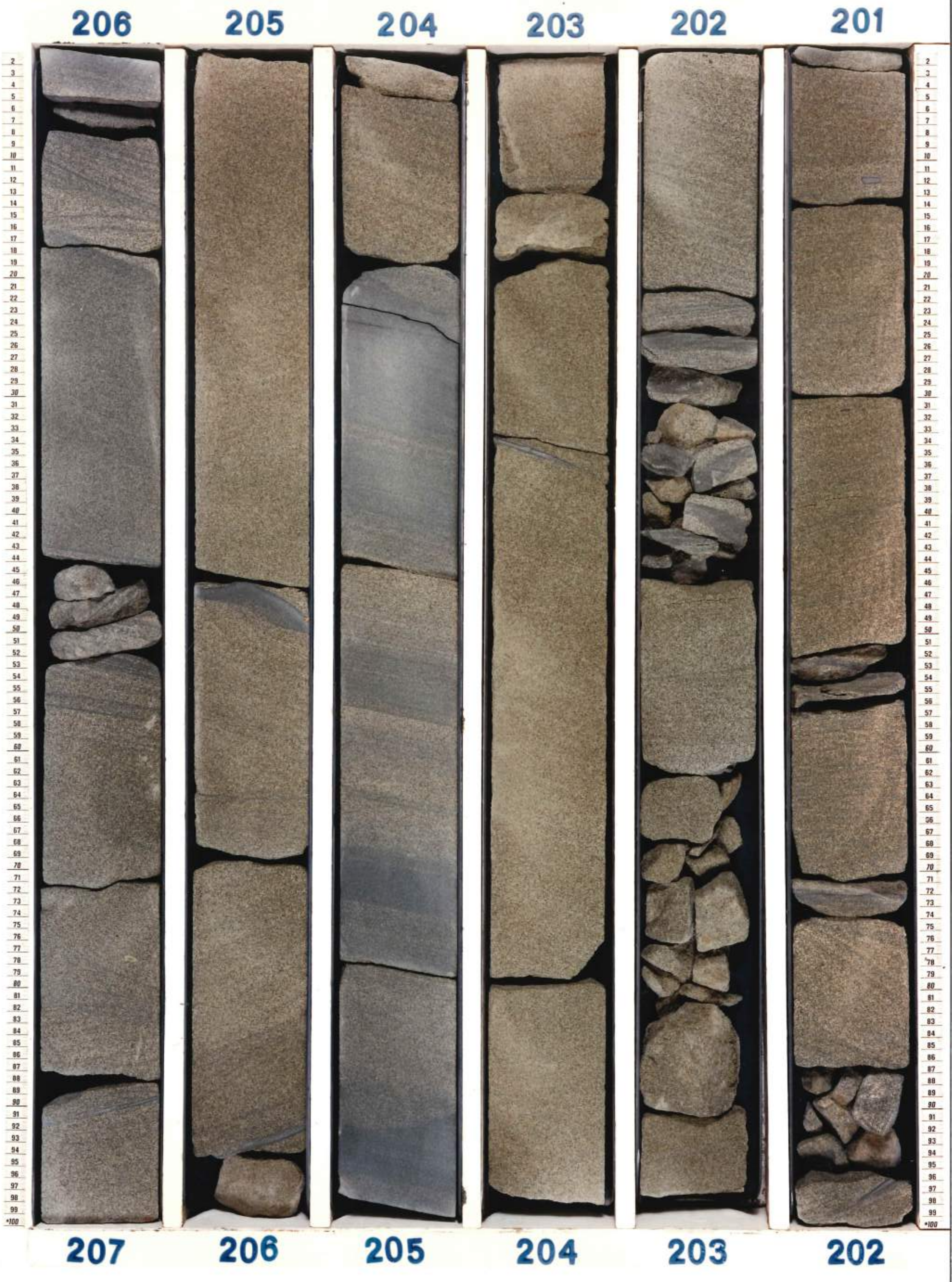


BOHRUNG
GURTEN
UNIVERSITÄT BERN 1989
212
211
210
209
208
207
213
212
211
210
209
208

UNIVERSITÄT BERN 1989

BOHRUNG GURTEN

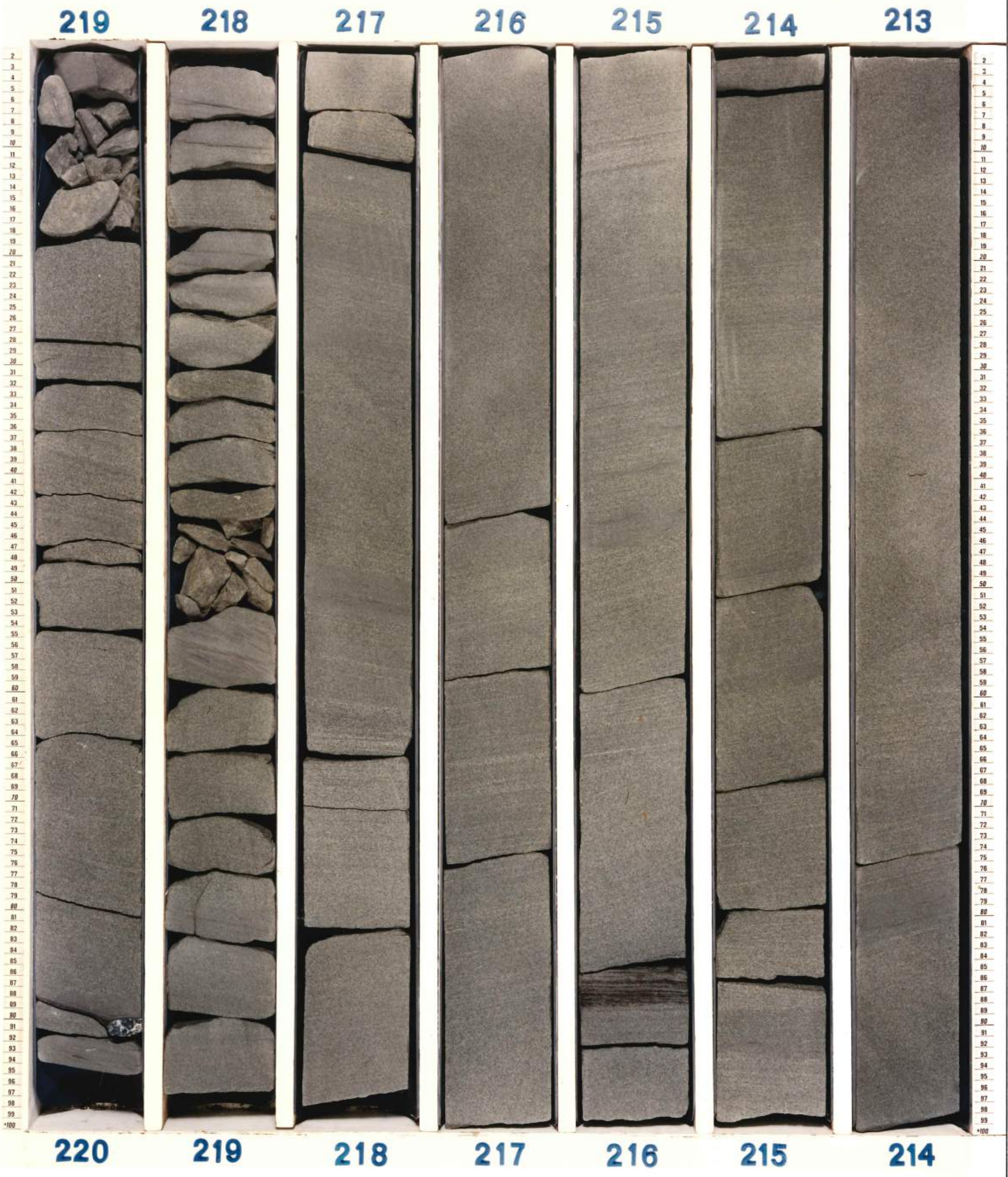

UNIVERSITÄT BERN 1989

BOHRUNG GURTEN

226 225 224 223 222 221 220

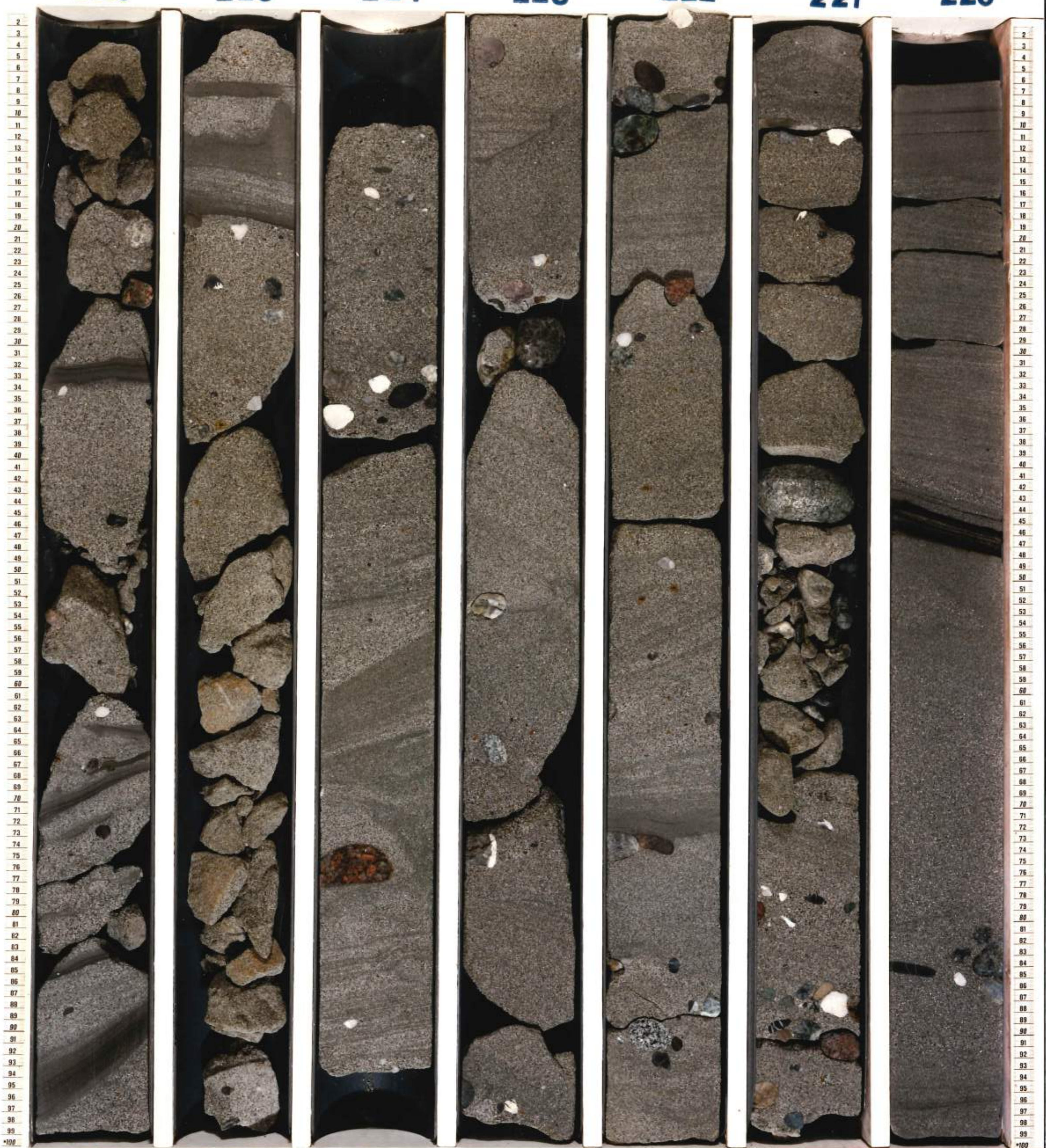

227 226 225 224 223 222 221

UNIVERSITÄT BERN 1989

BOHRUNG GURTEN

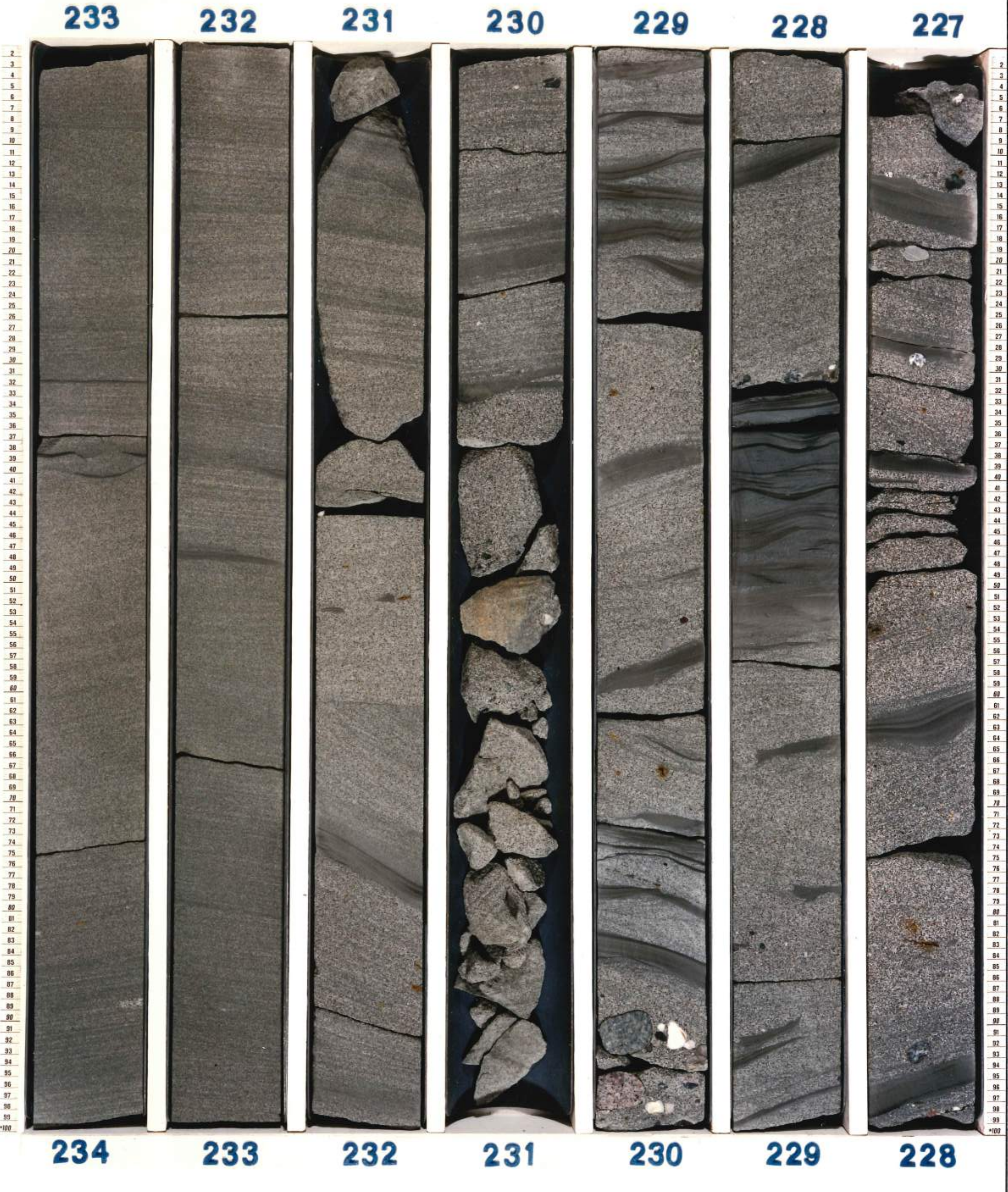

UNIVERSITÄT BERN 1989

BOHRUNG GURTEN

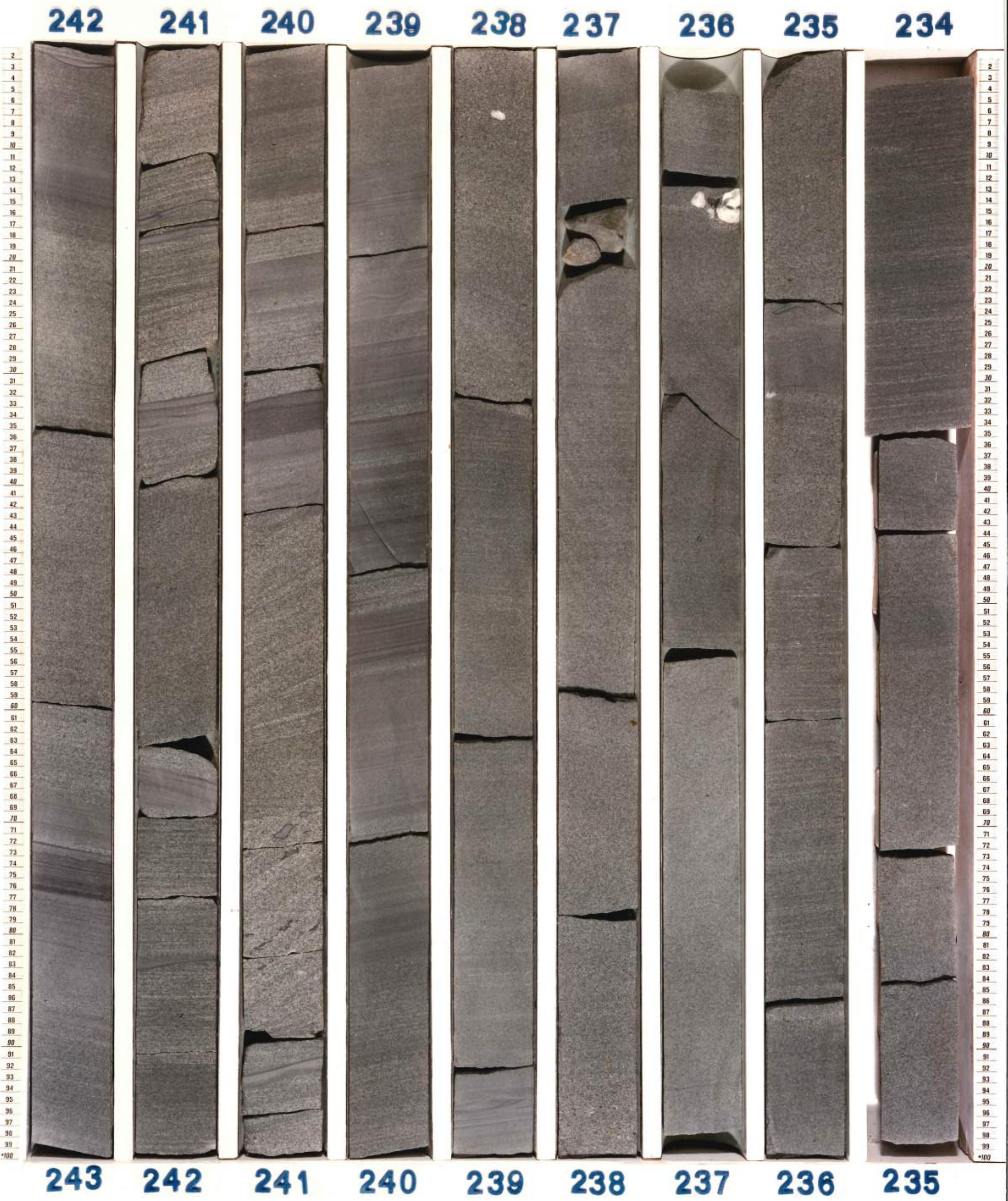

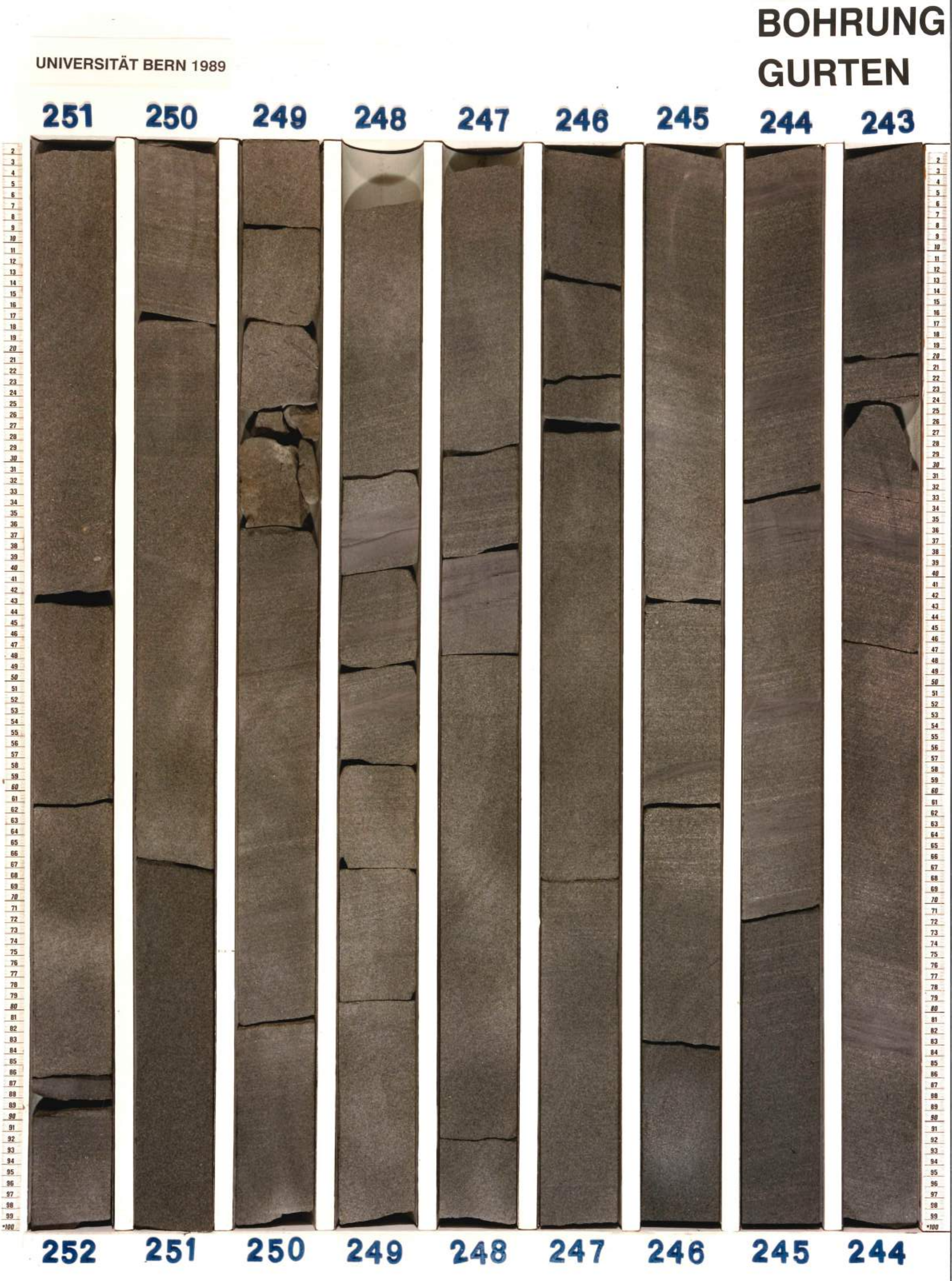
UNIVERSITÄT BERN 1989
BOHRUNG
GURTEN
251 250 249 248 247 246 245 244 243
252 251 250 249 248 247 246 245 244

BOHRUNG GURTEN

UNIVERSITÄT BERN 1989

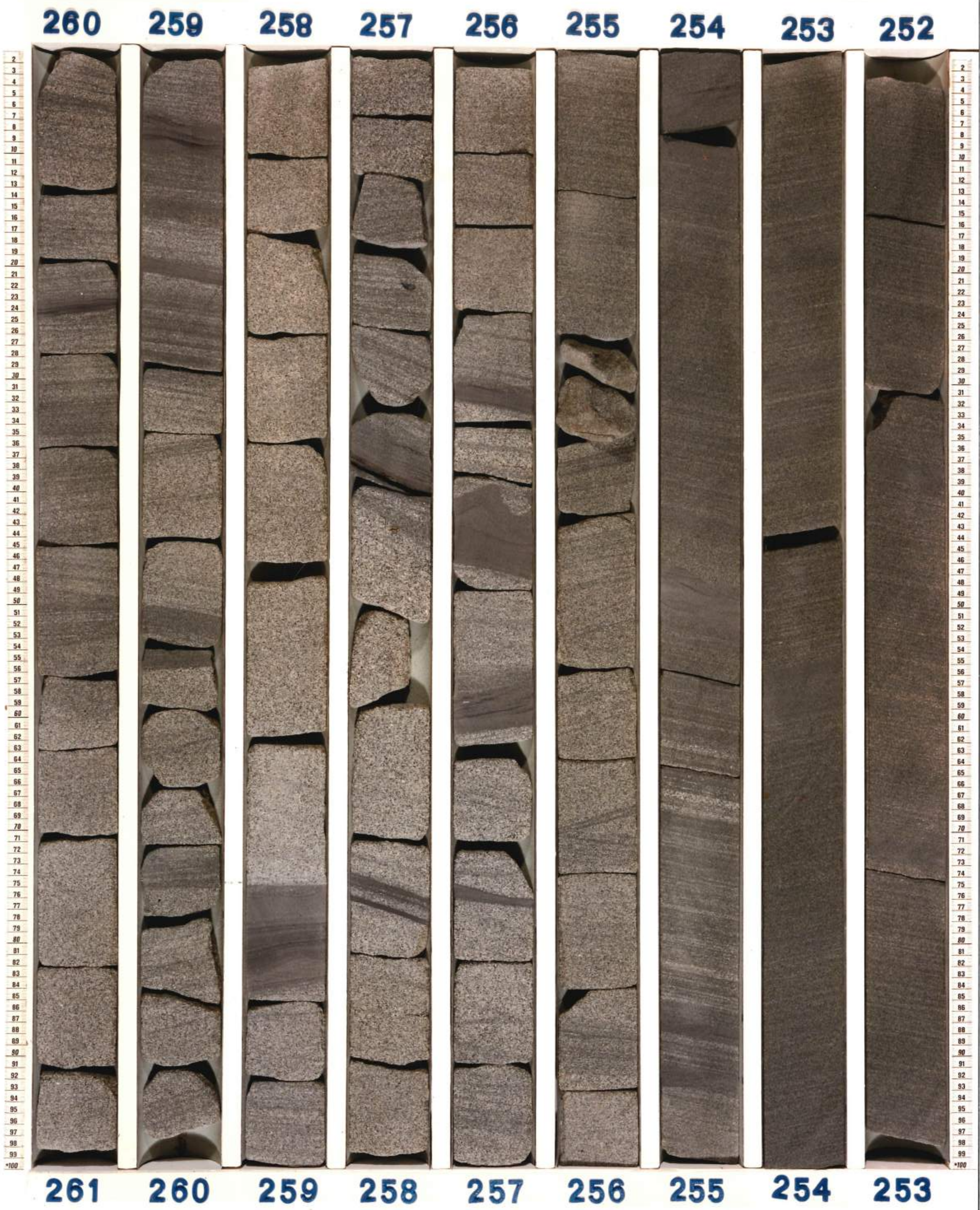

UNIVERSITÄT BERN 1989

BOHRUNG GURTEN